# Enhanced electromechanical response of Fe-doped ZnO films by modulating the chemical state and ionic size of the Fe dopant

J. T. Luo, Y. C. Yang, X. Y. Zhu, G. Chen, F. Zeng, and F. Pan*

*Laboratory of Advanced Materials, Department of Materials Science and Engineering, Tsinghua University, Beijing 100084, China*

(Received 19 May 2010; revised manuscript received 10 July 2010; published 29 July 2010)

To investigate the relationship between the electromechanical response, $d_{33}$, of doped ZnO and the dopant ionic size, the chemical state and ionic size of Fe in Fe-ZnO films were modulated through doping with various Fe concentrations and postannealing. We found that an enhanced $d_{33}$ of more than 110 pC/N is obtained in Fe-ZnO films when $Fe^{3+}$ with an ionic radius of 0.64 Å substitutes for the $Zn^{2+}$ (0.74 Å) site. The $d_{33}$ (less than 7 pC/N) is smaller than that of undoped ZnO films (11.6 pC/N) when $Fe^{2+}$ (0.76 Å) substitutes for $Zn^{2+}$. The enhanced electromechanical response is ascribed to polarization rotation induced by the external electric field. The microscopic origin is considered. Substitution of $Fe^{3+}$ with smaller ionic size for $Zn^{2+}$ results to the easier rotation of noncollinear Fe-O1 bonds along the $c$ axis under the applied field. Thus, the external electric field needed for polarization rotation is smaller. When bigger $Fe^{2+}$ substitutes for $Zn^{2+}$, rotation of Fe-O1 bonds becomes more difficult and thus the $d_{33}$ is smaller. A general mechanism is derived. Doping ZnO with a small ion produces enhanced electromechanical responses whereas doping ZnO with a big ion results in decreased electromechanical responses. This mechanism is useful for guiding the design of new wurtzite semiconductors with enhanced electromechanical responses.

DOI: 10.1103/PhysRevB.82.014116 PACS number(s): 77.84.Bw, 77.65.−j, 77.80.Fm, 77.55.−g

## I. INTRODUCTION

Zinc oxide (ZnO), a versatile material, has a growing technological importance because its many favorable properties.[1,2] One of the distinctive properties of ZnO is it exhibits the largest electromechanical response, $d_{33}$, among the known tetrahedral semiconductors,[3] making it suitable for devices in microelectromechanical and communication systems.[4] However, performances of the device might be restricted by its relatively small $d_{33}$ to some extent. As an important parameter evaluating electromechanical response, the $d_{33}$ value of ZnO is ~9.9 pC/N for a bulk and ~12.4 pC/N for an oriented film,[5,6] which is approximately one order of magnitude lower compared to common piezoelectric perovskite ceramics. Unfortunately, the high toxicity of lead in perovskite materials and the large lattice mismatch with silicon limit their application.[7] If the $d_{33}$ of nontoxic and simple-structured ZnO could be increased to be comparable with perovskite piezoelectrics, ZnO can be used as a candidate for lead-free piezoelectric materials and the performance of available ZnO-based devices can be qualitatively improved. Interestingly, we have obtained 2.5 at. % V-doped ZnO films ($Zn_{0.975}V_{0.025}O$) and 6 at. % Cr-doped ZnO films ($Zn_{0.94}Cr_{0.06}O$) with maximum $d_{33}$ values of ~170 and ~120 pC/N, respectively.[8,9] Using V-doped ZnO films as the piezoelectric layer, we have fabricated surface acoustic wave devices with improved performances.[10] Similar electromechanical response improvement can also be found in V-doped ZnO nanofibers.[11] In our previous works, we have also found that 2 at. % Cu-doped ZnO films have a $d_{33}$ of ~13.6 pC/N, and Fe- and Co-doped ZnO films with the same doping concentration have $d_{33}$ values of ~6 pC/N and ~11 pC/N, respectively.[12] Thus, the question that immediately emerges is why ZnO films doped with moderate V, Cr, and Cu have enhanced $d_{33}$ values, whereas ZnO films doped with 2 at. % Fe and Co have decreased $d_{33}$. Although V, Cr, and Cu dopants may improve crystallographic quality, and thus enhance $d_{33}$ more or less, because the undoped and V-, Cr-, and Cu-doped ZnO films are highly oriented, this effect becomes limited. Notably, V is in +5 oxidation state in $Zn_{0.975}V_{0.025}O$ and Cr is in +3 oxidation state in $Zn_{0.94}Cr_{0.06}O$. Both $V^{5+}$ (0.59 Å) and $Cr^{3+}$ (0.63 Å) radii are smaller than that of $Zn^{2+}$ (0.74 Å). In the corresponding TM-doped ZnO, Cu, Fe, and Co exist at the chemical state of +2. The sizes of $Fe^{2+}$ (0.76 Å) and $Co^{2+}$ (0.79 Å) are bigger than that of $Zn^{2+}$ but $Cu^{2+}$ (0.72 Å) is a little smaller. Therefore, one can hypothesize that the $d_{33}$ value of ZnO could be enhanced by doping it with a transition metal ion that is smaller than that of $Zn^{2+}$ whereas doping ZnO with a bigger sized ion may decrease its $d_{33}$. This mechanism, if correct, would be useful for guiding the design of new semiconductors with enhanced electromechanical responses. The chemical state of Fe in Fe-ZnO may be different at different conditions and Fe ionic size may be changed with a change of its chemical state in Fe-ZnO. Therefore, we chose Fe-ZnO films to verify this mechanism.

In this study, we report the tremendous difference in electromechanical response between $Zn_{0.988}Fe_{0.12}O$ and $Zn_{1-x}Fe_xO$ ($x \geq 2.6$ at. %) films. Postannealing in $O_2$ and $H_2$ ambience was performed to verify the relationship between the electromechanical response of Fe-doped ZnO and the size of the Fe ion.

## II. EXPERIMENT

A series of $Zn_{1-x}Fe_xO$ ($x$=0, 1.2, 2.6, 4, 5.6, and 7.4 at. %) films were deposited on Si (100) single-crystal substrates by direct current reactive magnetron cosputtering using a Zn target (99.99% purity, 120 mm diameter). Several Fe pieces (99.99% purity, 5 mm × 2 mm) were added uniformly around the sputtering race track. In order to adjust the concentration of Fe in the deposited films, the number of Fe

 

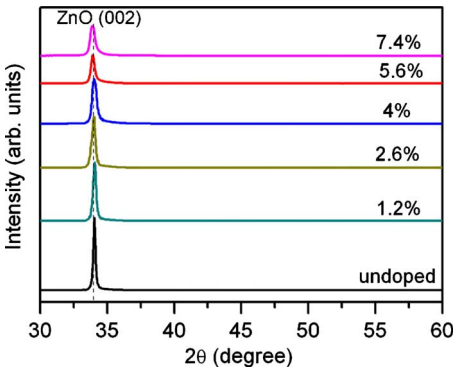


FIG. 1. (Color online) XRD patterns of $Zn_{1-x}Fe_xO$ ($x$=0, 1.2, 2.6, 4, 5.6, and 7.4 at. %) films.

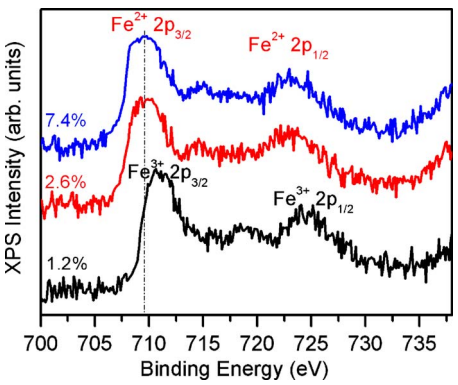


FIG. 2. (Color online) Fe 2$p$ XPS spectra of $Zn_{1-x}Fe_xO$ films ($x$=1.2, 2.6, and 7.4 at. %).

pieces in the sputtering area was varied. Substrates were placed parallel to the target surface at a distance of about 67 mm. The base pressure of the chamber was lower than $5 \times 10^{-4}$ Pa, and the working pressure was a mixture of Ar (0.3 Pa) and $O_2$ (0.5 Pa), which were controlled by two different flow meters. Presputtering was performed for 15 min to remove contaminations on the targets. The deposition rate was 0.05 nm/s and the substrate temperature during deposition was 200 °C. The thickness of the samples was ~280 nm, as measured by a stylus profiler. The Fe concentration was determined by induced coupled plasma atomic emission spectroscopy and confirmed by x-ray fluorescence. The microstructure of the films was characterized by x-ray diffraction (XRD) using Cu $K\alpha$ radiation (40 kV, 200 mA) with $\lambda$=1.5408 Å. Fe $L_{2,3}$ edge x-ray absorption spectrum (XAS) and x-ray photoelectron spectroscopy (XPS) were used to characterize the local environment of the Fe ion and its chemical state in ZnO films.

## III. RESULTS AND DISCUSSIONS

The XRD patterns of $Zn_{1-x}Fe_xO$ ($x$=0, 1.2, 2.6, 4, 5.6, and 7.4 at. %) films are shown in Fig. 1. A peak appears at ~34°, which corresponds to the (002) diffraction of the ZnO hexagonal wurtzite structure. All films are single-phased with a $c$-axis-preferred orientation, and no evidence of any other Fe secondary phases and impurities are detected. Compared with undoped ZnO films, there is a relative shift of the (002) peak to a lower angle for $Zn_{1-x}Fe_xO$ ($x \geq 2.6$ at. %), whereas $Zn_{0.988}Fe_{0.12}O$ has a relative shift of the (002) peak to a higher angle. A similar peak shift has also been observed in Co-doped ZnO and V-doped ZnO films.[13,14] Changes in the (002) diffraction peak indicate that Fe is incorporated into the wurtzite lattice. In addition, the relative intensity of the (002) diffraction peak decreases when Fe is doped into ZnO films, indicating that Fe deteriorates crystal quality.

The valence of Fe in ZnO:Fe films was characterized by XPS (Fig. 2). The Fe 2$p$ XPS spectrum of the $Zn_{0.988}Fe_{0.12}O$ film is different from that of $Zn_{1-x}Fe_xO$ ($x \geq 2.6$ at. %) films. The Fe $2p_{1/2}$ and Fe $2p_{3/2}$ peaks in the $Zn_{0.988}Fe_{0.12}O$ film are located at 724.7 eV and 710.6 eV, respectively, which are almost same as the values reported for $Fe_2O_3$:Fe $2p_{1/2}$ at 724.9 eV and Fe $2p_{3/2}$ at 710.7 eV.[15] A shake-up contribution at about 718.6 eV is consistent with available literature, which also indicate that Fe has a +3 oxidation state.[16] The Fe $2p_{3/2}$ and Fe $2p_{1/2}$ signals in the $Zn_{0.974}Fe_{0.026}O$ film are centered at 709.6 eV and 722.7 eV, respectively, which are very close to that of $Fe^{2+}$ in FeO (709.30 eV for Fe $2p_{3/2}$ and 722.3 eV for Fe $2p_{1/2}$) according to the handbook of XPS (Ref. 17) and previous reports.[18] With increasing Fe concentration, no significant change in chemical shift and signal was found for Fe $2p_{1/2}$ and Fe $2p_{3/2}$. Based on the XPS results, Fe in the $Zn_{0.988}Fe_{0.12}O$ film exists in the form of $Fe^{3+}$, whereas Fe chemical states in $Zn_{1-x}Fe_xO$ ($x \geq 2.6$ at. %) films are believed to be $Fe^{2+}$. The chemical state of Fe in Fe-ZnO films changes from $Fe^{3+}$ to $Fe^{2+}$ with an increase in the amount of Fe dopant, similar to that reported by other studies.[19,20]

Fe $L_{2,3}$ edge XAS obtained by the BL08U beam line of the Shanghai Synchrotron Radiation Facility was used to characterize the local environment and chemical states of Fe ion in Fe-ZnO films. The XAS spectra are highly sensitive to the valence state: an increase in the valence state of the transition metal ion by one causes a shift in the XAS $L_{2,3}$ spectra by 1 or more electron volt toward higher energies. The Fe $L_{2,3}$-edge XAS spectra of $Zn_{0.974}Fe_{0.026}O$, $Zn_{0.988}Fe_{0.012}O$, and $Zn_{0.974}Fe_{0.026}O$ annealed in $O_2$ are shown in Fig. 3. All Fe $L_{2,3}$ line shapes are consistent with a tetrahedral coordination, as expected of Fe ions substituting for Zn in the ZnO

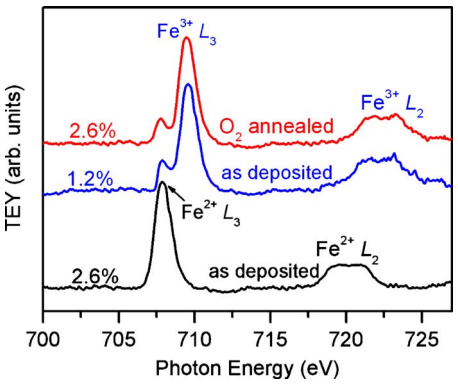


FIG. 3. (Color online) Room-temperature XAS spectra near Fe $L_{2,3}$ edges of $Zn_{1-x}Fe_xO$ films ($x$=1.2 and 2.6 at. %) and $Zn_{0.974}Fe_{0.026}O$ films annealed in $O_2$.

wurtzite lattice.[21] However, the XAS spectrum of $Zn_{0.974}Fe_{0.026}O$ is different from that of $Zn_{0.988}Fe_{0.12}O$.

Ferric oxide, which consists of trivalent Fe ions, is well known to exclusively exhibit doublet peaks at both $L_2$ and $L_3$ edges in its XAS spectrum.[22] The $Zn_{0.988}Fe_{0.12}O$ film shows a dominant peak near 710 eV, accompanied by double peaks near 721 and 723 eV, which are characteristic of $Fe^{3+}$ ions. The XAS spectrum of $Zn_{0.974}Fe_{0.026}O$ films does not show any doublet peak at both $L_2$ and $L_3$ edges. Peak positions for $L_2$ and $L_3$ edges are located at ~708 eV and ~720 eV, respectively, and have slightly lower photon energies than the corresponding $L$-edge peak position of $Fe_2O_3$. The line shape and $L$-edge peak position of $Zn_{0.974}Fe_{0.026}O$ films is coincident with that of FeO, indicating that Fe has a +2 oxidation state in $Zn_{0.974}Fe_{0.026}O$ films.[23,24] The Fe $L_{2,3}$-edge XAS spectrum of $Zn_{1-x}Fe_xO$ ($x > 2.6$ at. %) is the same as that of $Zn_{0.974}Fe_{0.026}O$ (not shown in figure). Therefore, $Fe^{3+}$ substitutes for Zn when Fe doping concentration is below 1.2 at. %. When the Fe doping concentration is above 2.6 at. %, $Fe^{2+}$ substitutes for Zn. From the above analysis and the XPS and XRD results, one can conclude that $Fe^{3+}$ successfully substitutes for the $Zn^{2+}$ site in the $Zn_{0.988}Fe_{0.12}O$ film whereas in $Zn_{1-x}Fe_xO$ ($x \geq 2.6$ at. %) films, $Fe^{2+}$ substitutes for the $Zn^{2+}$ site.

The electromechanical responses of films were characterized by a commercially available scanning probe microscope (SPM, Seiko Instruments SPI4000 & SPA300HV). Figure 4 shows the electromechanical response dependence of the applied voltage for $Zn_{0.988}Fe_{0.012}O$, $Zn_{0.974}Fe_{0.026}O$, and $Zn_{0.974}Fe_{0.026}O$ films annealed in $O_2$. Figure 4(a) shows that the $Zn_{0.988}Fe_{0.12}O$ film has a typical well-shaped displacement-voltage ($D$-$V$) butterfly loop with a displacement maximum of ~1.25 nm appearing at −8.9 V. This result shows a strain as high as 0.45% and indicates the ferroelectric behavior of the $Zn_{0.988}Fe_{0.12}O$ film. A similar ferroelectricity has also been observed in Li-doped ZnO systems.[25–27] A similar ferroelectricity in $Pb_{1-x}Ge_xTe$ and $PbS_xTe_{1-x}$ is ascribed to the following the phenomenon: when the size of the dopant ion is smaller than the host ion, the dopant ion can occupy off-center positions, thus locally inducing electric dipoles and resulting in ferroelectric behavior.[28,29] Glinchuk *et al.*[30] reported that the ferroelectricity of nonperovskite semiconductors, such as ZnO:Li, Be, and Mg, depends on a difference in the ionic size of the impurity and the host lattice ion as well as on the doping concentration. In the $Zn_{0.988}Fe_{0.012}O$ film, smaller $Fe^{3+}$ ions substitutes for $Zn^{2+}$ and occupies off-center positions, inducing ferroelectricity.

Every point on the $D$-$V$ curve is considered to contain information about piezoelectric deformation under the corresponding electric voltage. The electromechanical response hysteresis loop ($d_{33}$-$V$) can be calculated from the $D$-$V$ curve based on the law of converse piezoelectric effect. The $d_{33}$-$V$ loop clearly shows that the $Zn_{0.988}Fe_{0.12}O$ film is switchable and ferroelectricity is retained [Fig. 4(a)]. A maximum $d_{33}$ value of ~200 pC/N can also be found in Fig. 4(a). Considering that SPM characterization is a local method, measurements were conducted repeatedly on different points of $Zn_{0.988}Fe_{0.12}O$ films and an average $d_{33}$ (~127 pC/N) was obtained from over ten measurements. The value is comparable to the $d_{33}$ of some lead-free piezoelectric materials, making this a sort of lead-free and biocompatible piezoelectric material. The measured $d_{33}$ of undoped ZnO films in our work is 11.6 pC/N, which is in agreement with 12.4 pC/N for a similarly oriented film.[10] Thus, the average $d_{33}$ value for $Zn_{0.988}Fe_{0.12}O$ films is about one order of magnitude larger than that of undoped ZnO films. Although the improved crystallographic quality can increase $d_{33}$ value, the crystallographic quality of $Zn_{0.988}Fe_{0.12}O$ is not as good as the undoped ZnO film (Fig. 1). Therefore, the enhanced $d_{33}$ of $Zn_{0.988}Fe_{0.12}O$ cannot be ascribed to crystallographic quality improvement. A similar enhancement of the electromechanical response has also been observed in V- and Cr-doped ZnO systems.[8,9,11]

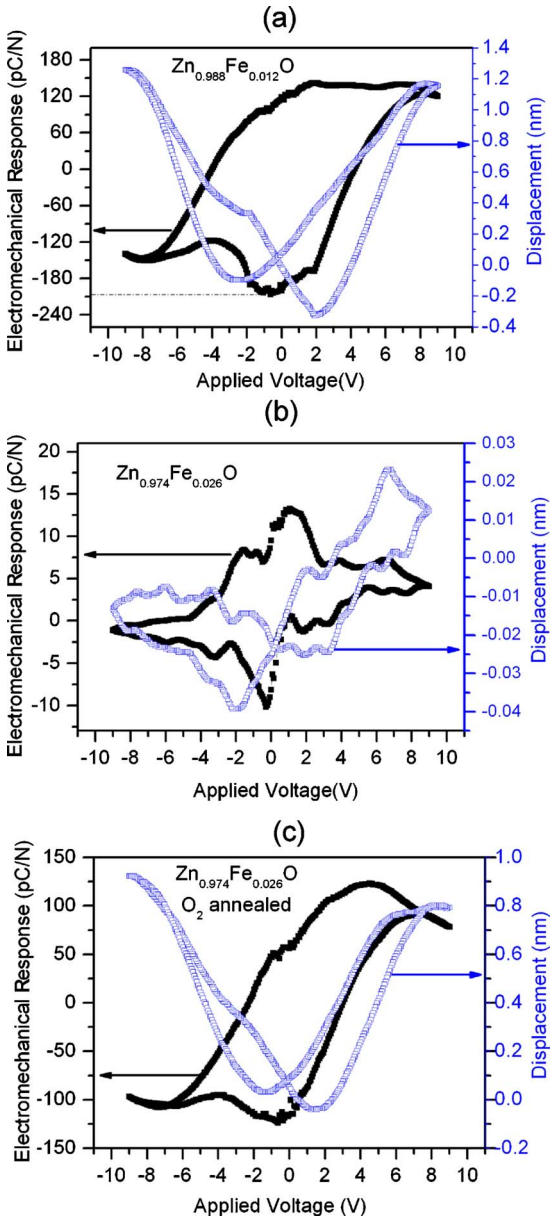


FIG. 4. (Color online) Displacement-Voltage ($D$-$V$) loop and the corresponding electromechanical response curve: (a) $Zn_{0.988}Fe_{0.12}O$ film, (b) $Zn_{0.974}Fe_{0.026}O$ film, and (c) $Zn_{0.974}Fe_{0.026}O$ annealed in $O_2$.

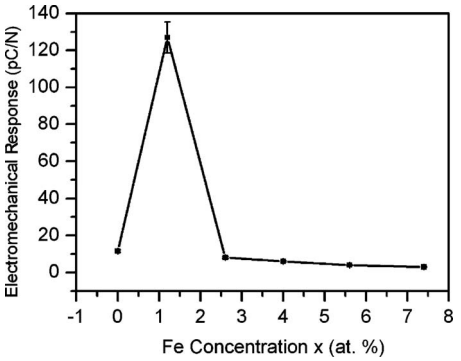


FIG. 5. The average electromechanical response $d_{33}$ as a function of Fe concentration $x$ in $Zn_{1-x}Fe_xO$ ($x$=0, 1.2, 2.6, 4, 5.6, and 7.4 at. %) films.

For the last two decades, the electromechanical responses of ferroelectric and piezoelectric perovskite oxides have been intensively studied.[31,32] Park *et al.*[33] reported that single-crystal $Pb(MgNb)O_3$-$PbTiO_3$ (PMN-PT) and $Pb(ZnNb)O_3$-$PbTiO_3$ (PZN-PT) solid solutions exhibit giant electromechanical responses on the order of ~2500 pC/N, which is about one order of magnitude higher than that of traditional piezoelectric ceramics. The enormous electromechanical response is ascribed to polarization rotation. The electric field applied noncollinearly along the pseudocubic [001], rather than in the rhombohedral [111] direction, causes polarization to rotate with much less energy, leading to a large strain response.[33,34] In this study, $Zn_{0.988}Fe_{0.12}O$ films also show ferroelectricity so a similar mechanism can be used to explain the remarkable electromechanical response in $Zn_{0.988}Fe_{0.12}O$ films. The phenomenological equation for $d_{33}$ can be expressed via a factor linking electrostrictive characteristics[35]

$$d_{33} = 2Q_{\text{eff}}\varepsilon_0\varepsilon_r P_s, \tag{1}$$

where $Q_{\text{eff}}$ is the effective electrostriction coefficient; and $P_s$, $\varepsilon_0$, and $\varepsilon_r$ are the spontaneous polarization, the permittivity of free space, and the relative permittivity, respectively. Ferroelectricity exists in $Zn_{0.988}Fe_{0.12}O$ films, and the spontaneous polarization, $P_s$, is switchable, which results in a large relative permittivity, $\varepsilon_r$.[36] Therefore, induced spontaneous polarization by $Fe^{3+}$ substitution in the $Zn_{0.988}Fe_{0.12}O$ film and the accompanying high permittivity are considered to be mainly responsible for the large electromechanical response.

SPM characterizations were also performed on $Zn_{0.974}Fe_{0.26}O$ films and the electromechanical response dependence of the applied voltage is shown in Fig. 4(b). The typical butterfly loop is not observed and the maximum displacement is less than 0.04 nm. The average electromechanical response of $Zn_{0.974}Fe_{0.26}O$ films from 10 measurements is 7 pC/N, which is smaller than that of undoped ZnO films (11.6 pC/N). To systematically investigate the electromechanical responses of Fe-doped ZnO films, SPM characterizations were also performed on films with other Fe concentrations. Figure 5 shows the average electromechanical response as a function of Fe concentration $x$ in $Zn_{1-x}Fe_xO$ films. Except for a significant enhancement of electromechanical response in $Zn_{0.988}Fe_{0.12}O$ films, all electromechanical responses in other Fe-doped ZnO films are smaller than that of undoped ZnO films because of structural deterioration (Fig. 1).

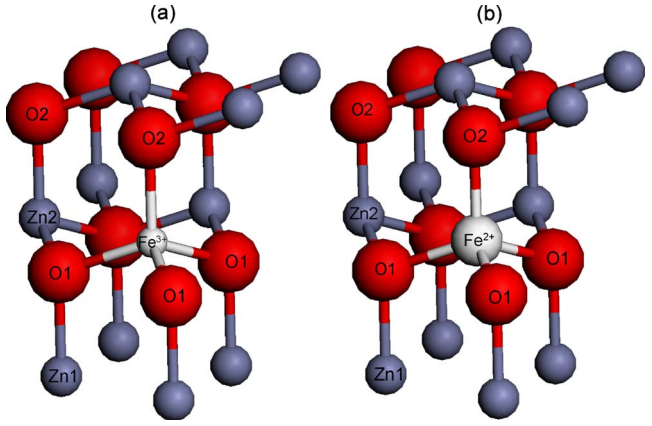


FIG. 6. (Color online) The $(2\times2\times1)$ supercell of Fe-doped ZnO system: (a) $Fe^{3+}$ substitutes for $Zn^{2+}$ site and (b) $Fe^{2+}$ substitutes for $Zn^{2+}$ site.

To date, the similar crystallographic qualities of $Zn_{0.974}Fe_{0.026}O$ and $Zn_{0.988}Fe_{0.12}O$ have been confusing because these have tremendously different electromechanical responses. Apparently, there are some intrinsic factors that result in a drastic difference in electromechanical response. Unfortunately, unlike the electronic properties of ZnO,[37,38] the electromechanical properties of these materials are poorly understood. Dal Corso *et al.* and Hill and Waghmare[39] reported piezoelectric constants ($e_{33}$) under zero field but the electromechanical coefficients ($d_{33}$) are the response of strain to a nonzero electric field. Karanth and Fu[40] studied the microscopic origin of the large electromechanical response in an undoped ZnO system under a nonzero electric field. They proposed that the large electromechanical response of ZnO originates from the strong coupling between strain and polarization. The dominant effect of the electric field in wurtzite semiconductors does not elongate the polar chemical bonds, as commonly believed. Rather, it serves to rotate the noncollinear bonds along the polar $c$ axis, i.e., Zn2-O1 bonds (Fig. 6), toward the direction of the applied field. This produces strain, which is the microscopic mechanism of a large electromechanical response in undoped ZnO. This suggests that the electromechanical response in wurtzite materials is mainly governed by ease of bond bending and rotation. This microscopic explanation also works in Fe-doped ZnO films with consideration of the rotation of Fe-O1 bonds, in addition to Zn2-O1 bonds (Fig. 6). Hence, the electromechanical response of our samples is mainly determined by the ease of Fe-O1 bond bending and rotation. In $Zn_{0.988}Fe_{0.12}O$ films, $Fe^{3+}$ ions substitute for $Zn^{2+}$ and the ionic radius of $Fe^{3+}$ (0.64 Å) is smaller than that of $Zn^{2+}$ (0.74 Å), which makes the switch of the $Fe^{3+}$-O1 bond toward the $c$-axis convenient. Moreover, $Fe^{3+}$ has a higher positive charge than $Zn^{2+}$ ions and noncollinear $Fe^{3+}$-O1 bonds have a stronger polarity than Zn2-O1 ones. Hence, $Fe^{3+}$-O1 bonds can rotate more easily under an applied field than Zn2-O1 ones [Fig. 6(a)]. This subsequently results in a large electromechanical re-

TABLE I. Electromechanical responses (pC/N) of $Zn_{1-x}Fe_xO$ ($x$=0, 1.2, and 2.6 at. %) films with a series of post treatments.

| Post treatment | $x$=0 | $x$=1.2 at. % | $x$=2.6 at. % |
|---|---|---|---|
| As deposited | 11.6 | 127 | 7 |
| Step 1 | 12.1 | 128 | 120 |
| Step 2 | 11.8 | 9 | 7 |
| Step 3 | 12 | 120 | 110 |

sponse according to the prediction of Karanth. On the other hand, $Fe^{2+}$ ions substitute for $Zn^{2+}$ in $Zn_{0.974}Fe_{0.026}O$ films and the ionic radius of $Fe^{2+}$ (0.76 Å) is larger than that of $Zn^{2+}$ [Fig. 6(b)], which make the rotation of $Fe^{2+}$-O1 bonds become more difficult than that of Zn2-O1. This is the reason why the electromechanical response is smaller than that of undoped ZnO films. Thus, one viewpoint can be deduced; the electromechanical response of ZnO can be enhanced when smaller $Fe^{3+}$, which has a higher positive charge, substitutes for $Zn^{2+}$ and decreases when bigger $Fe^{2+}$ substitutes for $Zn^{2+}$.

To further strengthen this argument, we modulated Fe chemical states and ionic sizes in $Zn_{1-x}Fe_xO$ ($x$=0, 1.2, and 2.6 at. %) films by a series of postannealing treatments at 500 °C for 60 min. Step 1, samples were annealed under $O_2$. Step 2, samples were annealed under $H_2$. Step 3, samples were again annealed under $O_2$. The electromechanical responses of all samples after each step were measured by SPM and the average electromechanical responses are shown in Table I. Although all samples possess improved electromechanical responses after the first step, as can be seen in line 3 of Table I, the increase in the electromechanical response of $Zn_{0.974}Fe_{0.026}O$ is remarkable. Postannealing may have improved the crystallographic quality and thus enhanced the electromechanical response more or less. Since both undoped ZnO and $Zn_{0.974}Fe_{0.026}O$ films are in the same condition, this effect should be the same for undoped ZnO and $Zn_{0.974}Fe_{0.026}O$ films. However, the increase in electromechanical response of $Zn_{0.974}Fe_{0.026}O$ (120 pC/N) is one order of magnitude larger than that of undoped ZnO (12.1 pC/N). Therefore, an increase in electromechanical response of $Zn_{0.974}Fe_{0.026}O$ seems to result from some other factor besides crystallographic quality improvement. Figure 4(c) shows the electromechanical response dependence of the applied voltage for $Zn_{0.974}Fe_{0.026}O$ film after Step 1. A typical well-shaped displacement-voltage ($D$-$V$) butterfly loop indicating the ferroelectric behavior of the $Zn_{0.974}Fe_{0.026}O$ film can be found in the figure. Hence, the enormous increase can be ascribed to spontaneous polarizations and the accompanying high permittivities. To investigate the changes in the chemical state and ionic size of Fe in the $Zn_{0.974}Fe_{0.026}O$ film after Step 1, XPS measurement was performed. Figure 7 shows the Fe 2$p$ spectrum of the as-deposited $Zn_{0.974}Fe_{0.026}O$ film after Step 1. The dominant chemical state of Fe ion changes from $Fe^{2+}$ to $Fe^{3+}$. A similar change in Fe chemical state can also be found in the Fe $L_{2,3}$ edge XAS shown in Fig. 3. Thus, after Step 1, $Fe^{3+}$ substitutes for the $Zn^{2+}$ site in $Zn_{0.974}Fe_{0.026}O$ films, and Fe ionic sizes become smaller than that of $Zn^{2+}$, which results in an easier rotation of the Fe-O1

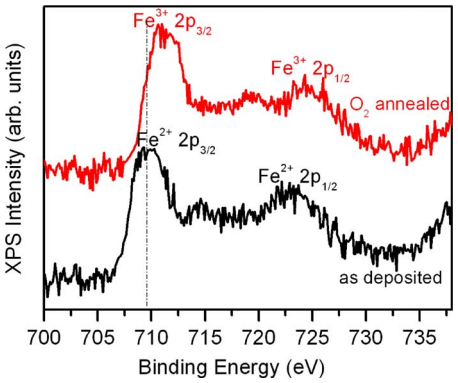


FIG. 7. (Color online) Fe 2$p$ XPS spectra of $Zn_{0.974}Fe_{0.026}O$ films as deposited and after Step 1 treatment.

bond [Fig. 6(a)]. As a result, the electromechanical response is significantly enhanced. On the other hand, after Step 2, the electromechanical responses of $Zn_{0.988}Fe_{0.12}O$ and $Zn_{0.974}Fe_{0.026}O$ films decrease dramatically, (Table I, line 4). From the Fe 2$p$ XPS spectra shown in Fig. 8, the $Fe^{2+}$ fraction increases at the cost of the $Fe^{3+}$ state, and the dominative valence of the Fe ion changes from $Fe^{3+}$ to $Fe^{2+}$ in $Zn_{0.988}Fe_{0.12}O$ films after Step 2. Therefore, $Fe^{2+}$ substitutes for the $Zn^{2+}$ site in the $Zn_{0.988}Fe_{0.12}O$ film, and the Fe ionic size becomes bigger than that of $Zn^{2+}$, resulting in a difficult rotation of the Fe-O1 bond. Accordingly, the electromechanical response decreases significantly. After Step 3, the dominant chemical state of Fe ion in $Zn_{0.988}Fe_{0.12}O$ films returns to $Fe^{3+}$ (Fig. 8) and the electromechanical response is again enhanced (Table I, line 5). The electromechanical response of the $Zn_{0.974}Fe_{0.026}O$ film is also enhanced. Thus, the electromechanical response of ZnO can be enhanced when smaller $Fe^{3+}$ ions substitute for $Zn^{2+}$ and decreased when bigger $Fe^{2+}$ ions substitute for $Zn^{2+}$. This is a general mechanism; that is, when smaller ions substitute for $Zn^{2+}$ in ZnO, they enhance electromechanical response, and when bigger ions substitute for $Zn^{2+}$ in ZnO, electromechanical responses decrease. Such a principle can be used for guiding the design of new wurtzite semiconductors with enhanced electromechanical responses.

It is easy to use this general mechanism to explain the question posed in the introduction. When moderate amounts

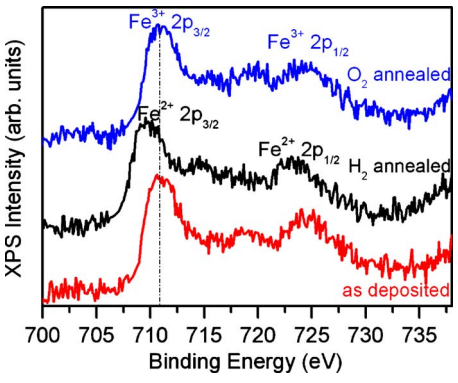


FIG. 8. (Color online) Fe 2$p$ XPS spectra of $Zn_{0.988}Fe_{0.012}O$ films as deposited after Step 2 and after Step 3 treatment.

of V, Cr, and Cu dope ZnO films, substitution of $V^{5+}$ (0.59 Å), $Cr^{3+}$ (0.63 Å), and $Cu^{2+}$ (0.72 Å) for $Zn^{2+}$ (0.74 Å) make the V-O1, Cr-O1, and Cu-O1 bonds rotate easier in the direction of the applied field and enhance the corresponding electromechanical responses. On the other hand, when 2 at. % Fe- and Co-doped ZnO films, a bigger ionic size in the $Zn^{2+}$ site makes the rotation of the Fe-O1 and Co-O1 bonds difficult and decreases the electromechanical response. Furthermore, the electromechanical responses in TM-doped ZnO and in piezoelectric single-crystals PMN-PT and PZN-PT have the same microscopic origin, i.e., polarization rotation. This is the key to understanding the electromechanical responses in tetrahedral semiconductors and in ferroelectric perovskites, which is significant in bridging these two seemingly unrelated fields.

## IV. CONCLUSION

In summary, we have developed a method of enhancing the electromechanical response of Fe-doped ZnO films by modulating the chemical state and ionic size of Fe dopant. An enhanced electromechanical response as high as 127 pC/N is obtained in $Zn_{0.988}Fe_{0.12}O$ films, whereas the electromechanical responses of $Zn_{1-x}Fe_xO$ ($x \geq 2.6$ at. %) films are smaller than that of undoped ZnO films. After annealing in $O_2$, the electromechanical response of the $Zn_{0.974}Fe_{0.026}O$ film increases up to 120 pC/N and the dominant chemical state of Fe changes from $Fe^{2+}$ to $Fe^{3+}$. On the other hand, the electromechanical response of the $Zn_{0.988}Fe_{0.12}O$ film decreases to 9 pC/N and the $Fe^{2+}$ fraction increases at the cost of the $Fe^{3+}$ state when it is annealed in $H_2$. The electromechanical response of doped wurtzite semiconductors and the ionic size of dopants is related in that the substitution of smaller dopant ions for the host ones enhances the electromechanical response and big dopant ion decrease the electromechanical response. The enhanced electromechanical responses make Fe-doped ZnO a promising candidate for lead-free, environment-friendly, and biocompatible piezoelectric materials.

## ACKNOWLEDGMENTS

We thank the SSRF for the local structure and chemical state measurements. This work was supported by National Hi-tech (R&D) Project of China (Grants No. 2007AA03Z426 and No. 2009AA034001), the National Natural Science Foundation of China (Grants No. 50871060 and No. 50772055), and the National Basic Research Program of China (Grant No. 2010CB832905).

*panf@mail.tsinghua.edu.cn

[1] Z. W. Pan, Z. R. Dai, and Z. L. Wang, Science **291**, 1947 (2001).
[2] F. Pan, C. Song, Y. C. Yang, X. J. Liu, and F. Zeng, Mater. Sci. Eng. R. **62**, 1 (2008).
[3] A. Dal Corso, M. Posternak, R. Resta, and A. Baldereschi, Phys. Rev. B **50**, 10715 (1994).
[4] T. Shibata, K. Unno, E. Makino, Y. Ito, and S. Shimada, Sens. Actuators, A **102**, 106 (2002).
[5] M. H. Zhao, Z. L. Wang, and S. X. Mao, Nano Lett. **4**, 587 (2004).
[6] J. A. Christman, R. R. Woolcott, Jr., A. I. Kingon, and R. J. Nemanich, Appl. Phys. Lett. **73**, 3851 (1998).
[7] C. L. Chen, H. H. Feng, Z. Zhang, A. Brazdeikis, Z. J. Huang, C. W. Chu, F. A. Miranda, F. W. Van Keuls, R. R. Romanofsky, and Y. Liou, Appl. Phys. Lett. **75**, 412 (1999).
[8] Y. C. Yang, C. Song, X. H. Wang, F. Zeng, and F. Pan, Appl. Phys. Lett. **92**, 012907 (2008).
[9] Y. C. Yang, C. Song, X. H. Wang, F. Zeng, and F. Pan, J. Appl. Phys. **103**, 074107 (2008).
[10] J. T. Luo, F. Zeng, F. Pan, H. F. Li, J. B. Niu, R. Jia, and M. Liu, Appl. Surf. Sci. **256**, 3081 (2010).
[11] Y. Q. Chen, X. J. Zheng, and X. Feng, Nanotechnology **21**, 055708 (2010).
[12] X. B. Wang, C. Song, D. M. Li, K. W. Geng, F. Zeng, and F. Pan, Appl. Surf. Sci. **253**, 1639 (2006).
[13] K. J. Kim and Y. R. Park, Appl. Phys. Lett. **81**, 1420 (2002).
[14] J. T. Luo, X. Y. Zhu, B. Fan, F. Zeng, and F. Pan, J. Phys. D **42**, 115109 (2009).
[15] T. Yamashita and P. Hayes, Appl. Surf. Sci. **254**, 2441 (2008).
[16] A. Gupta, A. Kumar, U. V. Waghmare, and M. S. Hegde, Chem. Mater. **21**, 4880 (2009).
[17] B. V. Crist, *Handbook of Monochromatic XPS Spectra: The Elements and Native Oxides* (Wiley, New York, 2000).
[18] P. Mills and J. L. Sullivan, J. Phys. D **16**, 723 (1983).
[19] L. M. Wang, J. W. Liao, Z. A. Peng, and J. H. Lai, J. Electrochem. Soc. **156**, H138 (2009).
[20] S. Kumar, Y. J. Kim, B. H. Koo, S. K. Sharma, J. M. Vargas, M. Knobel, S. Gautam, K. H. Chae, D. K. Kim, Y. K. Kim, and C. G. Lee, J. Appl. Phys. **105**, 07C520 (2009).
[21] P. Wu, G. Saraf, Y. Lu, D. H. Hill, R. Gateau, L. Wielunski, R. A. Bartynski, D. A. Arena, J. Dvorak, A. Moodenbaugh, T. Siegrist, J. A. Raley, and Y. K. Yeo, Appl. Phys. Lett. **89**, 012508 (2006).
[22] S. W. Ryu, J.-Y. Kim, Y.-H. Shin, B.-G. Park, Y. Son, and H. M. Jang, Chem. Mater. **21**, 5050 (2009).
[23] T. J. Regan, H. Ohldag, C. Stamm, F. Nolting, J. Lüning, J. Stöhr, and R. L. White, Phys. Rev. B **64**, 214422 (2001).
[24] J.-S. Kang, G. Kim, H. J. Lee, D. H. Kim, H. S. Kim, J. H. Shim, S. Lee, H. Lee, J.-Y. Kim, B. H. Kim, and B. I. Min, Phys. Rev. B **77**, 035121 (2008).
[25] M. Joseph, H. Tabata, and T. Kawai, Appl. Phys. Lett. **74**, 2534 (1999).
[26] N. J. Dhananjay and S. B. Krupanidhi, Appl. Phys. Lett. **89**, 082905 (2006).
[27] N. J. Dhananjay and S. B. Krupanidhi, J. Appl. Phys. **101**, 104104 (2007).
[28] Q. T. Islam and B. A. Bunker, Phys. Rev. Lett. **59**, 2701 (1987).
[29] Z. H. Wang and B. A. Bunker, Phys. Rev. B **46**, 11277 (1992).
[30] M. D. Glinchuk, E. V. Kirichenko, V. A. Stephanovich, and B. Y. Zaulychny, J. Appl. Phys. **105**, 104101 (2009).
[31] M. E. Lines and A. M. Glass, *Principles and Applications of*

*Ferroelectrics and Related Materials* (Clarendon Press, Oxford, 1979).
[32] R. E. Cohen, Nature (London) **358**, 136 (1992).
[33] S.-E. Park and T. R. Shrout, J. Appl. Phys. **82**, 1804 (1997).
[34] A. L. Kholkin, E. K. Akdogan, A. Safari, P.-F. Chauvy, and N. Setter, J. Appl. Phys. **89**, 8066 (2001).
[35] H. X. Fu and R. E. Cohen, Nature (London) **403**, 281 (2000).
[36] N. J. Dhananjay and S. B. Krupanidhi, J. Appl. Phys. **99**, 034105 (2006).
[37] O. Dulub, U. Diebold, and G. Kresse, Phys. Rev. Lett. **90**, 016102 (2003).
[38] A. Wander, F. Schedin, P. Steadman, A. Norris, R. McGrath, T. S. Turner, G. Thorton, and N. M. Harrison, Phys. Rev. Lett. **86**, 3811 (2001).
[39] N. A. Hill and U. Waghmare, Phys. Rev. B **62**, 8802 (2000).
[40] D. Karanth and H. X. Fu, Phys. Rev. B **72**, 064116 (2005).